GEOPHYSICAL RESEARCH LETTERS, VOL. ???, NO. , PAGES 1–4,

Noctilucent clouds, PMSE and 5-day planetary waves: a case study

S. Kirkwood, V. Barabash, B.U.E. Brändström, A. Moström, K. Stebel
Swedish Institute of Space Physics, Kiruna, Sweden

N. Mitchell
Department of Physics, University of Wales, Aberystwyth, Wales

W. Hocking
Department of Physics, University of Western Ontario, London, Ontario, Canada

Abstract. Analysis of global meteorological assimilations between mid-July and late-August 2000 shows strong 5-day planetary waves in the middle atmosphere. Observations of temperature, zonal wind, noctilucent clouds and polar mesosphere summer echoes (PMSE) near Kiruna, Sweden, all at heights between 80 and 95 km, show variations correlating with the passage of the 5-day waves. Temperature variations correlated with the 5-day wave reach 15 K peak-to-peak and correspond to modulation of PMSE occurrence by up to 50%. These observations appear to be the first experimental evidence of amplification of 5-day waves at the summer mesosphere which was predicted theoretically in 1976. A close linear relation is found between mean daily temperature and mean daily occurrence of PMSE. This can be explained if temperature is the primary factor controlling PMSE occurrence and time and height variations within each day between 80 and 90 km altitude reach 30 - 50 K.

1. Introduction

Noctilucent clouds (NLC) and polar mesosphere summer echoes (PMSE) are two phenomena characteristic of the very cold summer mesopause at high latitudes. Both are thought to be caused by aerosol formation, i.e. the formation of water-ice, when the temperatures fall low enough to cause saturation of the air (e.g. Gadsden and Schröder, 1989, Cho and Röttger, 1997). Very low temperatures arise at the summer high-latitude mesopause due to upwelling and expansion of air in an atmospheric circulation driven by breaking gravity waves (e.g. Andrews et al., 1987). Noctilucent clouds are considered to comprise rather large aerosols (size 40-1000 nm) and may require several hours or even days to form (Gadsden and Schröder, 1989) whereas the enhanced radar echoes, PMSE, are thought to be due to much smaller, charged aerosols or water cluster ions which should form more quickly. The mesopause temperature at a particular geographic location at a particular time will depend not only on the general circulation (upwelling) but also on perturbations caused by waves including gravity waves, planetary waves and tides. Here we focus attention on 5-day planetary waves which represent a well-known resonance in the atmosphere with longitudinal wave number 1 (e.g. Andrews et al., 1987).

Five-day periodicities have previously been reported in noctilucent clouds (Sugiyama et al., 1996) and in PMSE (Sugiyama et al., 1996, Kirkwood and Réchou, 1998). Kirkwood and Réchou proposed that temperature fluctuations associated with 5-day planetary waves could directly modulate the PMSE aerosol formation. In this paper we present new observations from a period of 40 days during late summer 2000. These allow us to demonstrate that 5-day planetary waves indeed propagate to mesopause heights, that they are strongly amplified there, and cause significant modulation of both PMSE and NLC.

Paper number .
0094-8276/02/$5.00

2. Observations

The period of study is 12 July - 22 August 2000, corresponding to day numbers 195-235. This represents the second half of the PMSE season and was selected on the basis of the distinct 5-day planetary-wave signatures in the global meteorological assimilations (see below). The various observations are summarized in Figure 1. All of the observations are made at, or close to the location of Esrange, near Kiruna in northern Sweden (67°53'N, 21°06'E).

Meteor winds are measured by the 32.5 MHz SkiYmet meteor radar located at Esrange (Mitchell et al., 2001). Winds have been derived from the Doppler shift of azimuth- and height- resolved echo returns from meteor trails. Horizontal winds have been derived by fitting a single value for each of zonal and meridional wind to all of the returns from each 24-hour period and 5-km height interval. The mean vertical wind is assumed to be zero. Results for the heights where most returns were observed are shown in the top (1st) panel of Figure 1. There is a clear trend as the summer wind minimum is steadily replaced by winter westerlies. Superimposed on the trend are quasi-periodic variations with periods 5-9 days.

Meteor temperatures are derived from height-resolved measurements of meteor-trail decay times from the same meteor radar as the winds. The decay time at heights 85-95 km decreases steadily with height. A reasonable first assumption is that this is primarily due to ambipolar diffusion, and so depends on temperature and neutral density, with the scale height of the neutral density depending on the temperature. With reasonable assumptions of temperature gradient, the neutral density and temperature contributions can be separated (for details see Hocking, 1999). Daily temperature estimates are plotted in the 2nd panel of Figure 1 and correspond to the height interval where most returns are observed, i.e. 85-95 km. There is a clear increasing trend during the interval plotted, as is to be expected at the end of the summer season. This is indicated by

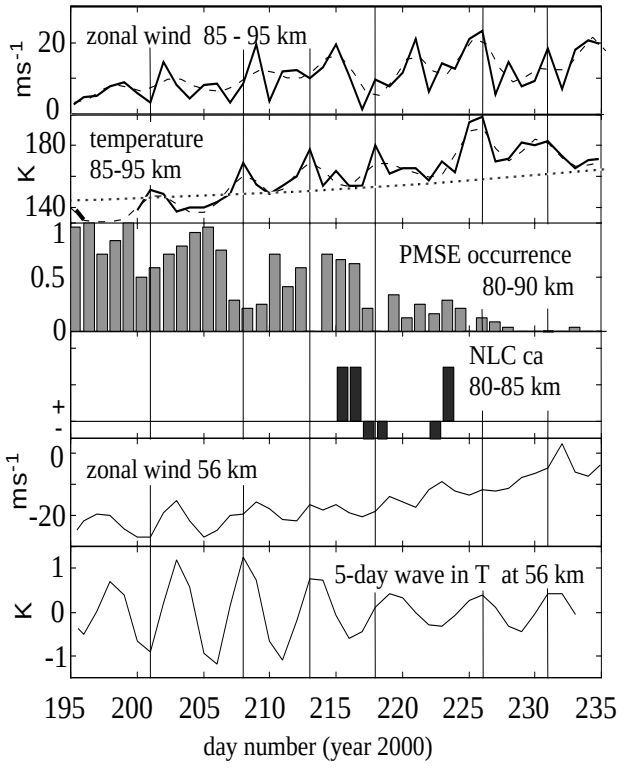

Figure 1. Observations 12 July to 22 August 2000. Top panel: daily average zonal winds from meteor radar, dashed line after low-pass filtering with 4-day cutoff; Second panel: temperature from meteor radar , dashed line after filtering with 4-day cutoff, dotted line temperatures from MSIS90E model ; Third panel: PMSE occurrence rate from ESRAD MST radar; fourth panel: observations of noctilucent clouds over N. Sweden; Fifth panel: zonal winds from UKMO assimilation ; Bottom panel: temperature perturbations associated with 5-day planetary waves from UKMO assimilation.

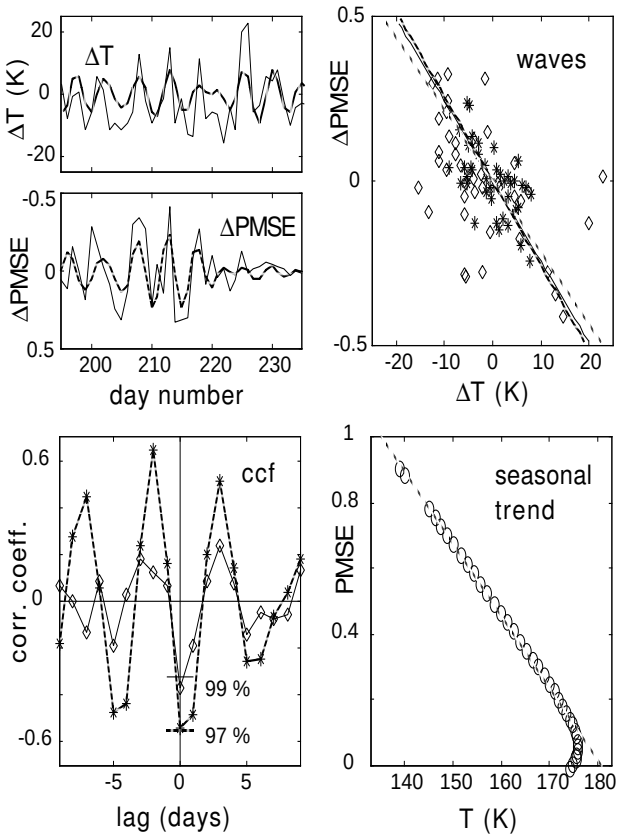

Figure 2. Relationship between temperature at 85-95 km (T) and the occurrence rate of PMSE. Panels 'ΔT' and 'ΔPMSE' show fluctuations after de-trending (solid line) and after filtering with 4-6 day band-pass (dashed lines). ΔPMSE is plotted with reversed sign. Panel 'ccf' shows cross correlations between ΔT and ΔPMSE - solid line with * for de-trended data, dashed line with ♢ for band-pass filtered data. 99 % and 97 % confidence limits are marked for the two ccfs, respectively. Panel 'waves' shows regression lines for de-trended (solid line and ♢) and band-pass filtered (dashed line and *) data. Regression line for seasonal trend is also shown (short-dashed line). Panel 'seasonal trend' plots the difference between the de-trended data and the original data (o), i.e. the seasonal trend in PMSE occurrence vs. the seasonal trend in T. Dashed line is a straight-line fit.

the dotted curve which shows corresponding temperatures from the MSIS90E empirical model (Hedin, 1991) which is based on large numbers of measurements by rockets and incoherent-scatter radar. There are also strong, quasi-periodic variations with 5-9 days period and amplitude about 10 K. The dates of peak temperatures are marked by vertical lines, which are repeated in all panels in Figure 1.

PMSE are recorded using the 52 MHz ESRAD radar at Esrange (Chilson et al., 1999). The measurements used here were made with 150 m height resolution, and 2 minute time resolution over the height interval 80-90 km. A 16-bit complementary code was used. The occurrence rate each day is computed on the basis of 1-hour by 2-km height bins. The percentage of bins with mean signal-to-noise ratio exceeding -10 dB is used to represent the occurrence rates, which are shown in the 3rd panel of Figure 1. A generally decreasing trend is seen over the period shown, as is normal at the end of the summer season. Superimposed on the trend there are rather large fluctuations with PMSE minima on days 200 and 208, with PMSE disappearing entirely on day numbers 213, 218 and 225, and PMSE reappearing on day 233 after several days with zero occurrence rates. Of the six temperature peaks marked in panel 2, 4 coincide with PMSE minima and two are on adjacent days to minima. The relationship between PMSE and temperature is further illustrated by Figure 2. Here the correlations in the seasonal trend, and in the fluctuations about the trend, are examined separately. Both the temperature and PMSE occurrence rates have been de-trended with a high-pass filter (cutoff at 50 days), as shown by the solid lines in the 'ΔT' and 'ΔPMSE' panels. The seasonal trend is then the difference between the de-trended data and the original data in Figure 1. In the 'seasonal trend' panel of Figure 2 a clear relationship between temperature and PMSE can be seen with PMSE occurrence rates falling from 100 % at about 130K-140 K to 0% at about 180 K. To extract the 5-day wave component, the observations have further been filtered with a 4-6 day band-pass filter, giving the dashed lines in the 'ΔT' and 'ΔPMSE' panels in Figure 2. The cross-correlation functions (panel 'ccf') show an anti-correlation with zero lag exceeding the 99% confidence level for the de-trended data, and the 97% confidence level for the band-pass filtered data. The dominance of the 5-day periodicity is seen clearly even in the unfiltered, de-trended data (solid ccf curve). Confidence intervals have been found by calculating 10000 cross-correlations with the real PMSE observations replaced by pseudo-data, comprising random selections from the original observations. The X% confidence level is the level exceeded at zero lag in (100-X)% of

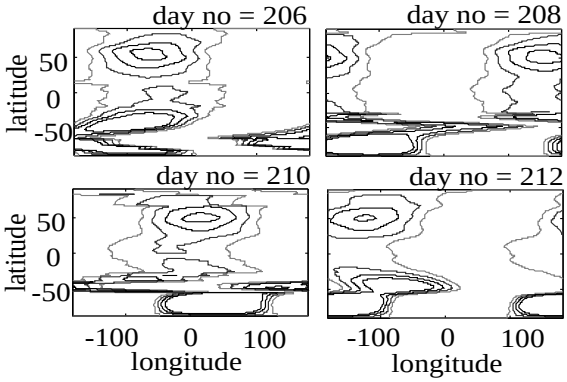

Figure 3. Temperature variations due to the 5-day planetary wave at the 0.5 mbar level (ca 56 km) between days 206 and 212 year 2000. Only the positive part of the wave is contoured for clarity. Contour lines correspond to 0, 0.3, 0.6 and 0.9 K.

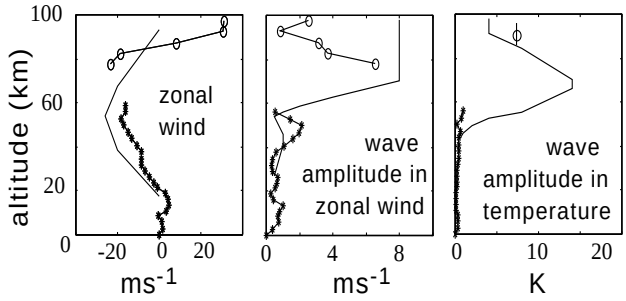

Figure 4. Comparison of modeling results from Geisler and Dickinson (solid line) with background winds and wave amplitudes from UKMO assimilations (*) and meteor radar (o) for day 215.

the random trials. Note that the application of the band-pass filter increases the correlation coefficient but slightly reduces the confidence. The 'waves' panel of Figure 2 shows the regression lines for the de-trended and band-pass filtered data. It can be seen that these are very close to each other, and to the PMSE/T dependence found from the seasonal trend.

Noctilucent cloud observations for the region where the PMSE were observed are available from a pair of automatic cameras operated from observatories about 400 km south of the radar site (from the towns Lycksele and Överklinten in Sweden, Stebel et al., 2000). These recorded the night sky with 1- minute time resolution from 1-25 August, allowing the presence or absence of NLCs directly over the radar site to be monitored whenever the sky was reasonably clear of tropospheric clouds. Note that before 1 August the night sky at such high latitudes is too light to allow observation of NLCs. The NLC observations are shown in the 4th panel of Figure 1. The results are shown by the black bars: positive for NLC present, negative for reasonably clear sky and NLC absent. Note that NLC occurrences are plotted per night rather than per day. The data are sparse but those NLC which are observed coincide with local maxima in PMSE occurrence rates. When information on the absence of NLCs is available, these coincide with periods of low or absent PMSE (nights 217/218, 218/219, 222/223).

Meteorological assimilations providing global wind, temperature and geopotential height fields are available from the British meteorological office, UKMO (Swinbank and O'Neill, 1994). The resolution of the assimilations is 2.5° in latitude, 3.75° in longitude and 22 pressure levels are available from 1000 to 0.3 mbar (ca 0 - 60 km altitude). One assimilation is available each day representing the situation at 12 UT. Zonal winds for the grid point closest to the radar site, for the 0.5 mbar level (ca 55 km) are shown in the 5th panel of Figure 1. They show the expected trend from the easterlies of summer towards westerlies of winter with a superimposed oscillation period 4-7 days, amplitude ca 5 m/s. The phase of the wind oscillations at 0.5 mbar seems to be the same as at 85-95 km (top panel) but the noisiness of the latter makes an exact comparison difficult.

We use the same meteorological assimilations as above to detect 5-day planetary waves. A Fourier transform of the values around each latitude circle is used to extract the wave number 1 component (complex amplitude). The time series of complex amplitudes for each latitude and pressure level is then filtered with a 4-6 day band-pass filter. The global temperature and wind fields corresponding to the wave perturbation each day can then be reconstructed using the filtered complex amplitudes. The results for temperature are illustrated by Figure 3 which shows the characteristic temperature maxima, one in the northern (summer) hemisphere, one in the southern (winter) hemisphere, migrating westward around the globe, taking about 5 days to complete the circuit. The results generally show coherent wave structures up to 0.5 mbar (ca 55 km).

Temperature fluctuations in the planetary wave at the 0.5 mbar level at the location of our radar site are shown in the 6th panel of Figure 1. The wave is large (amplitude 1.2 K) and lasts for several cycles with close to 5-day period particularly during the first part of our study interval. Five of the six temperature maxima coincide within 1 day with the temperature maxima at 85-95 km (2nd panel). The temperature oscillation at 0.5 mbar is also coherent with the wind oscillation at the same height.

3. Discussion and Conclusions

The technique for deriving temperatures from meteor trail diffusion times is new and not yet entirely proven. The close association we see, between temperature fluctuations measured by this technique and other parameters - particularly the fluctuations in occurrence of PMSE and the 5-day waves at 0.5 mbar - Figure 1, is a strong indication that the technique indeed is able to resolve temperature fluctuations on a day-to-day scale. However, we cannot rule out the possibility of systematic errors affecting the absolute temperature values. The close linear dependence of mean daily PMSE occurrence rate on mean daily temperature indicates that temperature is the primary parameter affecting PMSE occurrence. The observed 50 K span in mean daily temperatures between conditions giving 100% and 0% PMSE occurrence, respectively, implies a similar 50 K variability in temperatures at PMSE heights over each day, since PMSE has a strong daily variation , generally disappearing entirely in late evening (Kirkwood et al., 1995). The restriction of PMSE to the height interval 80-90 km suggests a similar temperature dependence since height variations in the mean daily temperature lie in the same range, i.e. they are about 30 K (Lübken, 1999). The daily variation and 100% hour-to-hour modulations which are often observed should then also correspond to similarly large temperature variations due to tides and shorter-period gravity waves. The demonstrated sensitivity of PMSE to temperature fluctuations associated with 5-day waves, supports the earlier suggestion by Kirkwood and Réchou (1998) that 5-day planetary waves significantly modulate ice-aerosol formation at mesopause heights. The NLC observations, although sparse, are also consistent with this suggestion.

According to the modeling work of Geisler and Dickinson (1976), the 5-day wave can be strongly amplified in the summer,

high-latitude mesosphere, with the amplification depending on the strength of the background zonal wind. According to the UKMO assimilations, zonal winds up to 60 km height at the beginning of August (day 215) are close to 'solstice' model in Geisler and Dickinson (1976). According to the model, maximum temperature wave amplitudes in the mesosphere should appear at about 70 km altitude and for the decreasing background winds during our study interval, increase from about 9 to 11 K between the start and end of the period.

In Figure 4 we compare our observations for the beginning of August with the model results. In the first panel we compare observed zonal winds with those used in the model. They are broadly similar. The second and third panels in Figure 4 compare the model and observed 5-day wave perturbations. For the wind perturbations, the agreement is reasonable, although our observations suggest attenuation above 80 km which is not shown in the model. For temperatures, we have only one point at high altitudes, but the agreement with the model is good where data is available.

We can conclude that we have observed strong amplification of 5-day planetary waves in the summer, high-latitude mesosphere in reasonable agreement with the predictions of Geisler and Dickinson (1976). This seems not to have been reported previously, perhaps understandably since continuous measurements of temperature are needed (24 hours a day to allow averaging of tidal effects and over several 10's of days to see the 5-day signal). Previously only optical methods have been available to measure temperatures at the summer polar mesosphere (primarily OH spectrometry and lidar) which are unable to satisfy these requirements. Large temperature changes (30 K) over a short time period (3-4 weeks) have been noted during autumn at mid-latitudes (Taylor et al., 2001) and stationary planetary waves have been proposed as the explanation (Liu et al., 2001). However, the planetary wave model used in the latter case was unable to produce such high amplitude variations as observed. Our study here, demonstrates rather that large temperature perturbations (at least 15 K peak to peak) are induced by the non-stationary 5-day planetary wave near the summer mesopause.

Acknowledgments. Meteorological data was provided by the British Atmospheric Data Center. The ESRAD MST radar is operated in cooperation with Swedish Space Corporation (Esrange) and this research has otherwise been funded by the Swedish Natural Science Research Council.

References

Andrews, D., J. Holton, and C. Leovy, *Middle Atmosphere Dynamics*, Academic Press, New York, 1987.

Chilson, P. B., S. Kirkwood, and A. Nilsson, The Esrange MST radar: A brief introduction and procedure for range validation using balloons, *Radio Sci.*, *34*, 427 – 436, 1999.

Cho, J., and J. Röttger, An updated review of polar mesosphere summer echoes: Observation, theory and their relation to noctilucent clouds and subvisible aerosols, *J. Geophys. Res.*, *102*, 2001 – 2020, 1997.

Gadsden, M., The north-west europe data on noctilucent clouds : a survey, *J. Atmos. Sol. Terr. Phys.*, *60*, 1163–1174, 1998.

Gadsden, M., and G. Schröder, *Noctilucent Clouds*, Springer Verlag, Berlin Heidelberg, 1989.

Geisler, J. E., and R. E. Dickinson, The five-day wave on a sphere with realistic zonal winds, *J. Atmos. Sci.*, *33*, 632–641, 1976.

Hedin, A. E., Extension of the MSIS thermosphere model into the middle and lower atmosphere, *J. Geophys. Res.*, *96*, 1159 – 1171, 1991.

Hocking, W. K., Temperatures using radar-meteor decay times, *Geophys. Res. Letters*, *26*, 3297 – 3300, 1999.

Kirkwood, S., J. Cho, C. M. Hall, U. P. Hoppe, D. P. Murtagh, J. Stegman, W. E. Swartz, A. P. vanEyken, G. Wannberg, G. Witt, A comparison of PMSE and other ground-based observations during the NLC-91 campaign, *J. Atmos. Terr. Phys.*, *57*, 35–44, 1995.

Kirkwood, S., and A. Réchou, Planetary wave modulation of PMSE, *Geophys. Res. Letters*, *25*, 4509–4512, 1998.

Liu, H.-L., R. Roble, M. Taylor, and W. P. Jr., Mesospheric planetary waves at northern hemisphere fall equinox, *Geophys. Res. Letters*, *28*, 1903–1906, 2001.

Lübken, F.-J., Thermal structure of the Arctic summer mesosphere, *J. Geophys. Res.*, *104*, 9135–9149, 1999.

Mitchell, N. J., D. Pancheva, H. Middleton, and M. Hagan, Mean winds and tides in the Arctic mesosphere and lower thermosphere, *J. Geophys. Res.*, *submitted*, 2001.

Stebel, K., V. Barabash, S. Kirkwood, J. Siebert, and K.-H. Fricke, Simultaneous and common-volume observations by radar, lidar and CCD camera, *Geophys. Res. Letters*, *27*, 661–664, 2000.

Sugiyama, T., Y. Murako, H. Sogawa, and S. Fukao, Oscillations in polar mesospheric summer echoes and bifurcation of noctilucent cloud formation, *Geophys. Res. Letters*, *23*, 653–656, 1996.

Swinbank, R., and A. O'Neill, A stratosphere-troposphere data assimilation system, *Monthly Weather Review*, *122*, 686–701, 1994.

Taylor, M., W. P. Jr., H.-L. Liu, C. She, L. Gardner, R. Roble, and V. Vasoli, Large amplitude perturbations in mesospheric OH Meinel and 87-km Na lidar temperatures around autumnal equinox, *Geophys. Res. Letters*, *28*, 1899–1902, 2001.

S. Kirkwood, Swedish Institute of Space Physics, P.O. Box 812, S-981 28 Kiruna, Sweden. (e-mail: sheila@irf.se)

(Received _____.)